# Carbon isotope (δ13Ccarb) and facies variability at the Wenlock-Ludlow boundary (Silurian) of the Midland Platform, UK

Blain, John Allan; Wheeley, James; Ray, David

*DOI:*
10.1139/cjes-2015-0194

# Carbon isotope ($\delta^{13}C_{carb}$) and facies variability at the Wenlock-Ludlow boundary (Silurian) of the Midland Platform, UK

John A. Blain[a*], David C. Ray[a] and James R. Wheeley[a]

[*]Corresponding author

[a]School of Geography, Earth & Environmental Sciences, University of Birmingham, Edgbaston, B15 2TT, United Kingdom;

[*] john.a.blain@gmail.com

daveray01@yahoo.com

j.r.wheeley@bham.ac.uk

**Abstract**

The Wenlock-Ludlow series boundary (Silurian) has been recognized as a time of pronounced sea level rise and the end of a globally recognised Late Homerian Stage (Mulde) positive carbon isotope excursion (CIE). However, the precise timing and synchronicity of the end of the excursion with respect to the Wenlock-Ludlow boundary is debated. Within the type Wenlock and Ludlow areas (UK), high resolution $\delta^{13}C_{carb}$ isotope data are presented across the Wenlock-Ludlow boundary, and within a range of carbonate platform settings. Correlation between sections and depositional settings has been based upon the characteristics of high-order sea level fluctuations (parasequences). Comparisons between parasequence bounded $\delta^{13}C_{carb}$ values reveal clear spatial variations, with lighter values recorded from more distal settings and heavier values from shallower settings. Temporal variations in the $\delta^{13}C_{carb}$ values are also documented and appear to reflect local variations in carbonate provenance and productivity in response to sea level rise. While $\delta^{13}C_{carb}$ values converge in all sections towards the Wenlock-Ludlow boundary, the apparent end of the Mulde CIE appears diachronous and is progressively older within more distal settings.

**Keywords:** Carbon Isotopes, Carbonate Platform, Mulde, Sea Level, Silurian.

## Introduction

The Silurian is characterised by a highly dynamic, glacially mediated climate, associated with strong eustatic sea level fluctuations, marine biodiversity crises and carbon isotope excursions (CIE) (Calner 2008; Munnecke *et al*. 2010; Melchin *et al*. 2012). Four prominent positive CIEs are recognized within the Silurian (the Ireviken (Early Sheinwoodian), Mulde (Late Homerian), Lau (Ludfordian) and Klonk (Silurian-Devonian Boundary) events, see Saltzman & Thomas 2012) and are increasingly used as a means of stratigraphic correlation (Cramer *et al.* 2011). The Homerian Stage of the Wenlock Series is associated with the double-peaked and globally recognised Mulde positive CIE; the upper peak of which occurs in the latest Homerian, with elevated $\delta^{13}C_{carb}$ values continuing towards the Wenlock-Ludlow boundary. In addition, the Wenlock-Ludlow boundary is associated with a well-established, globally recognised transgression that likely begins in the very latest Homerian and peaks in the middle Gorstian (Ludlow Series) (Loydell 1998; Johnson 2006; Johnson 2010; Melchin *et al*. 2012).

Within the southern United Kingdom, Wenlock and Ludlow age strata are exposed on the Midland Platform and the eastern part of the Welsh Basin (Cherns *et al.* 2006). These exposures, particularly those of the Midland Platform, are of global significance in that they contain the Global boundary Stratotype Sections and Points (GSSPs) for the constituent stages of the Wenlock (Sheinwoodian and Homerian) and Ludlow (Gorstian and Ludfordian) series. A compilation of key sections produced for the British Geological Conservation Review Series (Aldridge *et al*. 2000), and more recently, a field guide for the International Subcommision on Silurian Stratigraphy (Davies *et al*. 2011), provide details of the type Wenlock and Ludlow series.

The GSSP for the base of the Gorstian Stage is in Pitch Coppice Quarry near the town of Ludlow, Shropshire (SO 472 730). The stratotype point is the base of the Lower Elton Formation (LEF) where it overlies the Much Wenlock Limestone Formation (MWLF) (Lawson & White 1989). Graptolites questionably assigned to *Neodiversograptus nilssoni* Zone have been collected immediately above the base of the LEF. However, the absence of graptolites from other parts of the Homerian-Gorstian interval in the type area, alongside an absence of biostratigraphically useful shelly fossils, conodonts and palynomorphs, make it impossible to precisely correlate the stratotype point with the base of *N. nilssoni* Zone; the base of *N. nilssoni* Zone being globally used to recognise the base of the Gorstian (Melchin *et al*. 2012). In light of this biostratigraphic imprecision, carbon isotope chemostratigraphy may help improve correlation of the Homerian-Gorstian boundary. However, while the upper peak of the Mulde CIE is reported from the MWLF at Pitch Coppice Quarry (Corfield *et al*. 1992; Thomas & Ray 2011), both regionally (Marshall *et al*. 2012) and globally (Cramer *et al*. 2006), the precise relationship between the Homerian-Gorstian boundary and the upper peak of the Mulde CIE is unclear.

In an attempt to improve the correlation of the Homerian-Gorstian boundary on the Midland Platform, recent studies have focussed on sequence stratigraphy (Ray *et al*. 2010; Ray *et al*. 2013), and the stable isotope record (Cramer *et al*. 2012). In particular, detailed studies of the relative sea level changes within upper MWLF and immediately overlying LEF have identified a series of highly distinctive and regionally traceable parasequences. These parasequences can be traced across much of the northern and central Midland Platform and are documented within the type Wenlock (Wenlock Edge, Shropshire) and type Ludlow (Ludlow anticline, Shropshire) areas (Ray *et al*. 2010; Thomas & Ray 2011). Furthermore, within these same areas, $\delta^{13}C_{carb}$ determinations have identified the upper peak of the Mulde CIE (Corfield *et al*. 1992; Marshall *et al*. 2011; Marshall *et al*. 2012). Based upon the regional correlation of the declining $\delta^{13}C_{carb}$ values, Marshall *et al*. (2012) identified a diachronous end to the Mulde positive CIE. In particular, elevated and regionally anomalous, $\delta^{13}C_{carb}$ values were reported 6m into the LEF at Lea South Quarry, Wenlock Edge. These values were attributed, in part, to locally high carbonate productivity and or upwelling taking place close to the shelf-basin margin. If correct, such diachroneity would cast doubt on the use of CIEs as a means of high resolution correlation.

Presented herein are three sections containing the MWLF-LEF boundary interval, the associated parasequences and the declining upper limb of the Mulde CIE. Together these sections represent a platform to platform margin transect, as developed within the type Wenlock and Ludlow areas. Such sections allow for the regional expression of the Mulde CIE to be compared against sequence stratigraphic determinations and across differing palaeoenvironments.

## Lithostratigraphy and sequence stratigraphy

The transition between the MWLF and LEF has been investigated along Wenlock Edge at Benthall Edge Quarry (SJ 664 034) and Lea South Quarry (SO 594 982), and at Goggin Road (SO 472 719), Ludlow (Fig. 1). While these sections do not contain useful age diagnostic fossils, parasequence based correlations have been used to link to nearby sections that do. Age diagnostic graptolites corresponding to the latest Homerian *M. ludensis* Zone are regionally reported from the upper MWLF and *N. nilssoni* Zone graptolites are reported from the LEF (see Aldridge *et al*. 2000; Ray *et al*. 2010). Based upon regional palaeoenvironmental considerations, during late Homerian times, (Shergold & Bassett 1970; Scoffin 1971; Ray *et al*. 2010) Benthall Edge and Lea South quarries corresponded to patch reef and barrier reef settings (reef tract), respectively, while Goggin Road corresponded to a platform margin setting (off-reef tract) (Aldridge *et al*. 2000; Thomas & Ray 2011). In terms of relative sea level change, the upper MWLF is associated with a marked relative sea level fall (falling stage systems tract) corresponding to parasequence 10 (PS10) of Ray *et al.* (2010) and the widespread establishment of reefs and shallow-water carbonates. The overlying parasequence 11 (PS11) marks the onset of regional transgression, resulting in localised reefal build-ups and shoals in areas of high carbonate productivity (Lea South Quarry), and, more widely, the onset of the drowning of the carbonate platform (Benthall Edge Quarry and Goggin Road). The commencement of the LEF is typically associated with parasequences 12 to 15 (PS11 locally) and sees the rapid and progressive replacement of carbonates by off-shore shales. Minor diachroneity of the MWLF-LEF boundary along Wenlock Edge reflects the lithological criteria originally established by Murchison (1872), which ties the top of the MWLF to the top of the crinoidal grainstone beds. Owing to local variations in carbonate productivity, the occurrence of the last prominent crinoidal grainstone beds varies from the top of PS10 at Benthall Edge to PS11 at Lea South Quarry (see Ray *et al.* 2010). Within the Ludlow area the replacement of limestones by shales defines the MWLF-LEF boundary and occurs at the top of PS11. The correlation of parasequences between all three sections has been based upon their distinguishing characteristics, which include shale-rich flooding surfaces overlain by upward-shallowing limestones (as determined on sedimentological and faunal grounds). In particular, PS10 is by far the thickest of the parasequences observed (>9 m) and is also the most strongly progradational, with a range of lithofacies representing environments from the lower limits of storm wave base and the euphotic zone to around fair-weather wave base. Above the lithological transition into the LEF begins with the locally variable PS11, above which a marked shift from carbonates to off-shore shales occurs at the transition between PS11 and PS12 and the Homerian-Gorstian Boundary. Thus correlation has been achieved by the identification of PS10 and overlying succession of thinner and dominantly retrogradational parasequences (Fig. 2).

## Carbon Isotope Stratigraphy

Each section was logged and sampled at 0.4m intervals, increasing to 0.2 m around the Wenlock-Ludlow boundary. Up to 2 mg of carbonate rock powder, per sample, was analysed using the University of Birmingham's SILLA laboratory facility. This method of analysing bulk rock for stable isotopes, which inevitably does contain some skeletal material, has been shown to provide reliable results in other Silurian studies (e.g. Cramer *et al*. 2006; Marshall *et al*. 2012; Jarochowska *et al*. In Press). The powdered carbonate was placed in a vial in a heated sample rack (90$^{o}$C), where the vial head space was replaced by pure helium via an automated needle system as part of an Isoprime Multiflow preparation system. Samples were then manually injected with approximately 200 µl of phosphoric acid and left to react for at least 1 hour before the headspace gas was sampled by an automated needle and introduced into a continuous-flow Isoprime mass-spectrometer. Duplicate samples were extracted from each vial and a mean value obtained for both $\delta^{13}C$ and $\delta^{18}O$. Samples were calibrated using IAEA standards NBS-18 and NBS-19 and reported as ‰ on the VPDB scale. An external precision of better than 0.1 ‰ is typically achieved for both $\delta^{13}C$ and $\delta^{18}O$. In total, 100 samples provided results (Table S1[1]).

Goggin Road is 1.1 km south of the Gorstian GSSP (Pitch Coppice) and appears lithologically rather similar. The section contains the upper third of PS10 and the majority (2.4 m) of PS11 (PS10 and PS11 are c.12 m and 2.14 m thick at Pitch Coppice; Thomas & Ray 2011), with the base of the LEF and the Gorstian Stage just above the top of the current exposure (PS11-PS12 boundary). Within the basal 1.8 m of the Goggin Road section, $\delta^{13}C_{carb}$ values show limited variability and fluctuate between +1.00 ‰ and +1.71 ‰ (mean +1.39 ‰). Above which, the remainder of the values are generally lower (mean +0.58 ‰) and show considerably more variability (+1.41 ‰ to -0.76 ‰). Minor positive shifts in values are observed towards the tops of PS10 and PS11.

Lea South Quarry contains the uppermost part of PS10, PS11 and the majority of PS12. The MWLF-LEF and Homerian-Gorstian boundary coincides with the top of the thickest crinoidal beds and here occurs at the top of PS11. $\delta^{13}C_{carb}$ values show a steady decline throughout (+2.99 ‰ to +1.23 ‰), with a minor peak (+3.4 ‰ at 2.3 m) close to the base of PS11, and a minor fall (+0.9 ‰ at 11.3 m) and plateau in values around the base of PS12.

[1] Table S1 – Stable isotope results *(supplementary material)*.

Benthall Edge Quarry contains the upper half of PS10, PS11 and part of PS12. The MWLF-LEF boundary coincides with the top of the thickest crinoidal beds and here occurs at the top of PS10 (Ray *et al*. 2010). Within upper half of PS10, $\delta^{13}C_{carb}$ values gently rise from around +2 ‰ to a peak of +3.35 ‰. Values then rapidly fall towards the top of PS10 with a value of +1.76 ‰ at the PS10-PS11 boundary (6.6 m). Above, PS11 values plateau, fluctuating between +1.58 ‰ and +2.04 ‰, before falling and plateauing again (+1.09 ‰ to +1.32 ‰) across the boundary between PS11 and PS12 and the Homerian-Gorstian stages.

## Discussion

$\delta^{13}C_{carb}$ values obtained from the three sections have been compared with respect to their relative positions within PS10, PS11 and PS12 (Fig. 3). Such a comparison reveals clear spatial variations with lighter $\delta^{13}C_{carb}$ values recorded from more distal settings and heavier values from shallower settings. Such a relationship is well documented within the Silurian and has been demonstrated in near age equivalent successions on Baltica (Jarochowska & Munnecke 2015). This is particularly evident in the mean $\delta^{13}C_{carb}$ values from PS11; Goggin Road +0.7 ‰, Lea South Quarry +2.6 ‰, Benthall Edge Quarry +1.8 ‰. The difference between sections is the likely result of local variations in carbonate provenance, biological activity and sea water circulation (see Saltzman & Thomas 2012). At Goggin Road, the limestones likely result from a mixture of in situ and derived carbonates; as is the case at Benthall Edge Quarry. As Goggin Road represents the most distal of the sections, in situ carbonate production will likely reflect the lighter $\delta^{13}C_{carb}$ values more typical of the open ocean, while carbonates derived from shallower-water carbonate production will be somewhat heavier. A particularly notable feature of PS11 at Goggin Road, and to a lesser extent Pitch Coppice (Thomas & Ray 2011), is the variability of $\delta^{13}C_{carb}$ values. Such variations may reflect pulses of platform derived carbonate deposited during storm events. This mechanism in combination with the relative sea level falls associated with individual parasequences, may also explain the minor positive shifts in values observed towards the top of PS10 and PS11. By way of contrast, Lea South Quarry is exclusively representative of shallow-marine in situ carbonate productivity and contains the highest mean $\delta^{13}C_{carb}$ values within PS11. Here, reef masses flanked by crinoidal grainstones are a common feature. The steady decline in $\delta^{13}C_{carb}$ values throughout PS11 reflects the best documentation of the declining limb of the Mulde CIE, with a minor fall and plateau in values around the base of PS12 likely corresponding to the end of the CIE; at a value of around +1 ‰. It is of note that a very similar carbon isotopic trend, including a plateau in values around +1 ‰, was produced by Marshall *et al*. (2012), however the plateau in values and the apparent end of the Mulde CIE does not occur until some 6m into the LEF (PS14). However by comparing the relative positions of the same Lea South Quarry isotope data between Marshall *et al.* (2011) and Marshall *et al.* (2012), it is clear there has been a degree of uncertainty as to the exact position of the data with respect to the stratigraphy at Lea South Quarry. Owing to such issues particular care has been taken in this study to correctly attribute isotopic values to the appropriate parasequences.

Spatial variations in $\delta^{13}C_{carb}$ values make the identification of the end of the Mulde CIE difficult. Within Benthall Edge Quarry, the steady decline in $\delta^{13}C_{carb}$ values observed at Lea South Quarry appears to correspond only to the upper 2.2 m of PS10, above which values plateau just below +2 ‰ in PS11, before falling and plateauing again around +1 ‰, across the PS11-PS12 boundary. Based upon the start of plateauing values, the end of the Mulde CIE might be attributed here to the base of PS11, or perhaps by comparison with the Lea South carbon isotope curve, near the top of PS11. At Goggin Road the identification of the end of the Mulde CIE is especially difficult, but may correspond to the transition between slightly elevated values with limited variability, and values that are generally lower and show considerably more variability, which occurs 2.2 m below the top of PS10.

However, the lowered $CaCO_3$ content within the uppermost MWLF at Goggin Road and the negative shift in $\delta^{13}C_{carb}$ values may reflect meteoric diagenetic processes. To test for the effects of diagenetic overprinting $\delta^{13}C_{carb}$ values were plotted against $\delta^{18}O$ values for each section (see Saltzman & Thomas 2012). There is no correlation between $\delta^{13}C_{carb}$ and $\delta^{18}O$ values at Lea South Quarry and Goggin Road (r2 = 0.0087 and 0.0483, respectively), while Benthall Edge Quarry comparisons suggest a weak correlation between values (r2 = 0.2975). Furthermore, at the level of individual samples diagenetic overprinting may be indicated by coinciding low $\delta^{13}C_{carb}$ and $\delta^{18}O$ values. Such coinciding values appear in samples from Benthall Edge Quarry (6.6 m) and Goggin Road (2.0 m and 4.8 m) (Fig. 3) and include samples attributed to the end of the Mulde CIE in both sections. However, in both sections the broader trends in values remain and indicate that the end of the Mulde CIE occurs well within PS10 at Goggin Road and in association with the onset of plateauing values in PS11 at Benthall Edge Quarry. Of additional note is the apparent absence of diagenetic overprinting at Lea South Quarry, the most shallow-water/proximal section, making meteoric digenesis as a result of subaerial exposure within the more distal sections highly unlikely, and suggesting a primary carbon isotopic signal for Benthall Edge Quarry and Goggin Road sections. Thus, according to the age control afforded by the parasequences, the end of the Mulde CIE appears to occur within progressively older strata within more distal settings. More broadly there is a convergence of values within all sections towards the PS11-PS12 and the Wenlock-Ludlow boundary, which may be interpreted as corresponding to the true end of the Mulde CIE; at a value of around +1 ‰. However, the PS11-PS12 boundary also corresponds to a marked increase in the rate of transgression, resulting in the widespread establishment of a more distal depositional setting which may have had the effect of lowering $\delta^{13}C_{carb}$ values and regionally bringing to an end the Mulde CIE.

**Acknowledgements**

We wish to thank Wayne Davies (Natural England) and Nicola Cowell (Mortimer Forest, Forestry Commission), Katy Bickerton (Edge Renewables), Cadi Price (Severn Gorge Wildlife Trust) and Ernest Carter (Aggregate Industries) for granting access and sampling permissions for Goggin Road and Lea South Quarry sections respectively. JRW dedicates his contribution to this work to June Everitt (1923–2012). We wish to thank Jiri Frýda and an anonymous reviewer for their helpful comments. This is a contribution to the International Geoscience Programme (IGCP) Project 591 - The Early to Middle Palaeozoic Revolution.

**References**

Aldridge, R.J., Siveter, David J., Siveter, Derek J., Lane, P.D., Palmer, D. & Woodcock, N.H. 2000. British Silurian Stratigraphy, Geological Conservation Review Series, No. 19, Joint Nature Conservation Committee, Peterborough, 542 pp.

Calner, M., 2008. Silurian global events – at the tipping point of climate change. *In* Mass Extinctions. *Edited by* A.M.T. Elewa. Springer-Verlag, Berlin and Heidelberg. pp. 21–58.

Cherns, L., Cocks, L.R.M., Davies, J.R., Hillier, R.D., Waters, R.A., Williams, M. 2006. Silurian: the influence of extensional tectonics and sea level changes on sedimentation in the Welsh Borderland

and on the Midland Platform. *In* The Geology of England and Wales. *Edited by* P. J. Brenchley and P. F. Rawson. The Geological Society, London, pp. 75–102.

Cramer, B.D., Kleffner, M.A., Saltzman, M.R. 2006. The Late Wenlock Mulde positive carbon isotope excursion in North America. GFF, **128:** 85–90.

Cramer, B.D., Brett, C.E., Melchin, M.J., Männik, P., Kleffner, M.A., McLaughlin, P.I., Loydell, D.K., Munnecke, A., Jeppsson, L., Corradini, C., Brunton, F.R., Saltzman, M.R. 2011. Revised correlation of Silurian Provincial Series of North America with global and regional chronostratigraphic units and $\delta^{13}C_{carb}$ chemostratigraphy. Lethaia, **44:** 185–202.

Cramer, B.D., Condon, D.J., Söderlund, U., Marshall, C., Worton, G.W., Thomas, A.T., Calner, M., Ray, D.C., Perrier, V., Boomer, I., Patchett, P.J., Jeppsson, L. 2012. U-Pb (zircon) age constraints on the timing and duration of Wenlock (Silurian) paleocommunity collapse and recovery during the 'Big Crisis'. Geological Society of America Bulletin, **124:** 1841–1857.

Corfield, R.M., Siveter, D.J., Cartlidge, J.E., McKerrow, W.S. 1992. Carbon isotope excursion near the Wenlock-Ludlow, (Silurian) boundary in the Anglo-Welsh area. Geology, **20:** 371-374.

Davies, J.R., Ray, D.C., Thomas, A.T., Loydell, D.K., Cherns, L., Cramer, B.D., Veevers, S.J., Worton, G.J., Marshall, C., Molyneux, S.G., Vandenbroucke, T.R.A., Verniers, J., Waters, R.A., Williams M., Zalasiewicz, J.A. 2011. Siluria revisited: A field guide. International Subcommission on Silurian Stratigraphy, Field Meeting 2011 (*Edited by*. D.C. Ray), 1–170.

Jarochowska, E., Munnecke, A. 2015. Silurian carbonate high-energy deposits of potential tsunami origin: Distributing lateral redeposition and time averaging using carbon isotope chemostratigraphy. Sedimentary Geology, **315**: 14-28.

Jarochowska, E., Munnecke, A., Frisch, K., Ray, D.C., Castagner, A. In press: Faunal and facies changes through the mid Homerian (late Wenlock, Silurian) positive carbon isotope excursion in Podolia, western Ukraine. Lethaia. Online publication DOI:10.1111/let.12137

Johnson, M.E. 2006. Relationship of Silurian sea-level fluctuations to oceanic episodes and events. GFF, **128:** 115–121.

Johnson, M. E. 2010. Tracking Silurian eustasy: Alignment of empirical evidence or pursuit of deductive reasoning? Palaeogeography, Palaeoclimatology, Palaeoecology, **296**: 276–284

Lawson, J.D., White, D.E. 1989. The Ludlow Series in the type area. *In* A Global Standard for the Silurian System. *Edited by* C. H. Holland and M. G. Bassett. National Museum of Wales, Geological Series, Cardiff. pp. 73-90.

Loydell, D.K. 1998. Early Silurian sea-level changes. Geological Magazine, **135:** 447–471.

Marshall, C., Thomas, A.T., Ray, D.C. 2011. Reef and inter-reef facies in the Much Wenlock Limestone Formation and overlying Lower Elton Formation, Lea Quarry South, Wenlock Edge. *In* Siluria Revisited, a Field Guide. *Edited by* D. C. Ray. International Subcommission on Silurian Stratigraphy Field Meeting 2011. pp. 113-120.

Marshall, C., Thomas, A.T., Boomer, I., Ray, D.C. 2012. High resolution δ13C stratigraphy of the Homerian (Wenlock) of the English Midlands and Wenlock Edge. Bulletin of Geosciences, **87:** 669-679.

Melchin, M.J., Sadler, P.M., Cramer, B.D. 2012. The Silurian Period. *In* The Geologic Time Scale 2012. *Edited by* F. M. Gradstein, J. G. Ogg, M. Schmitz, G. Ogg. Elsevier, New York. pp. 525–558.

Munnecke, A., Calner, M. Harper, D.A.T. Servais, T. 2010. Ordovician and Silurian sea–water chemistry, sea level, and climate: A synopsis. Palaeogeography, Palaeoclimatology, Palaeoecology, **296:** 389–413.

Murchison, R. I. 1872. Siluria. The history of the oldest known rocks containing organic remains, with a brief description of the distribution of gold over the Earth, 5th ed. John Murray, London:, xvi - 523 pp.

Ray, D.C., Brett, C.E., Thomas, A.T., Collings, A.V.J. 2010. Late Wenlock sequence stratigraphy in central England. Geological Magazine, **147:** 123–144.

Ray, D.C., Richards, T.D., Brett, C.D., Morton, A., Brown, A.M. 2013. Late Wenlock sequence and bentonite stratigraphy in the Malvern, Suckley and Abberley Hills, England. Palaeogeography, Palaeoclimatology, Palaeoecology, **389:** 115–127.

Saltzman, M.R., Thomas, E. 2012. Carbon Isotope Stratigraphy. *In* The Geologic Time Scale 2012. *Edited by* F. M Gradstein, J. G. Ogg, M. Schmitz, G. Ogg. Elsevier, New York. pp. 207-232.

Scoffin, T.P. 1971. The conditions of growth of the Wenlock reefs of Shropshire (England). Sedimentology, **17:** 173-219.

Shergold, J.H., Bassett, M.G. 1970. Facies and faunas at the Wenlock/Ludlow boundary of Wenlock Edge, Shropshire. Lethaia, **3:** 113-42

Thomas, A.T., Ray, D.C. 2011. Pitch Coppice: GSSP for the base of the Ludlow Series and Gorstian Stage, Whitwell Coppice. *In* Siluria Revisited, a Field Guide. *Edited by* D. C. Ray. International Subcommission on Silurian Stratigraphy Field Meeting 2011. pp. 80-84.

**Figure 1.** An outcrop map of the Much Wenlock Limestone Formation showing the location of sections and facies belts.

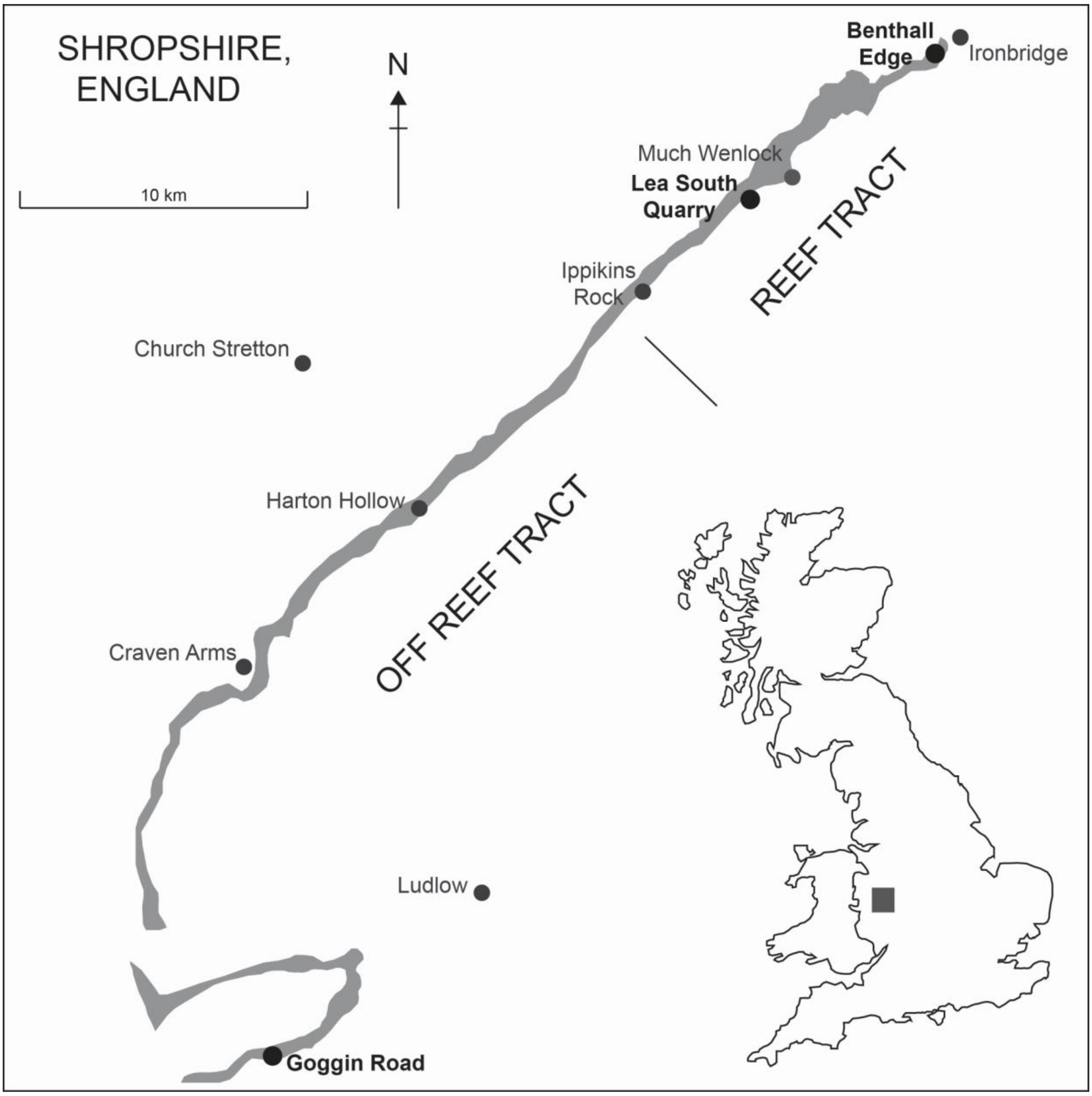


**Figure 2.** Key lithostratigraphy, sedimentology, parasequences and $\delta^{13}C_{carb}$ data from Goggin Road, Lea South Quarry and Benthall Edge Quarry. CMS – carbonate mudstone; WS – wackestone; PS – packstone; GS – grainstone. MWLF – Much Wenlock Limestone Formation; LEF – Lower Elton Formation.

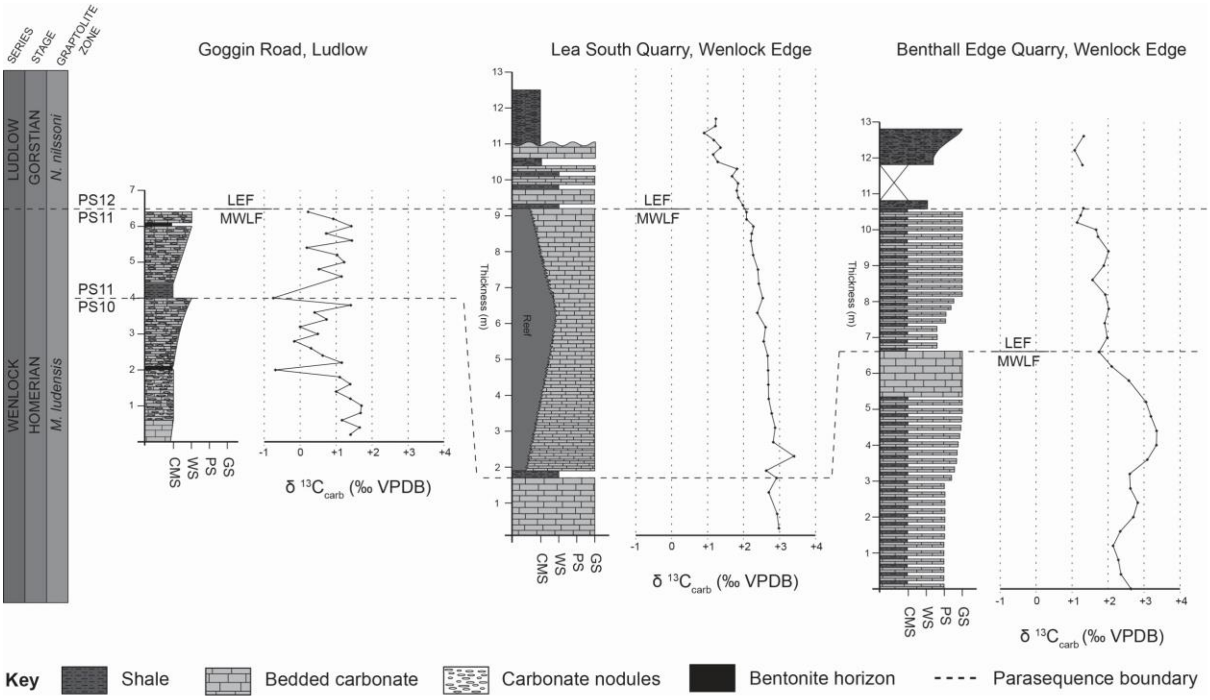


**Figure 3.** A comparison of $\delta^{13}C_{carb}$ between Goggin Road, Lea South Quarry and Benthall Edge Quarry with respect to the relative position of values within parasequences 10 to 12. Circled data points represent apparent end of the Mulde CIE in each section. Unshaded data points correspond to samples which may have been affected by meteoric diagenetic processes.

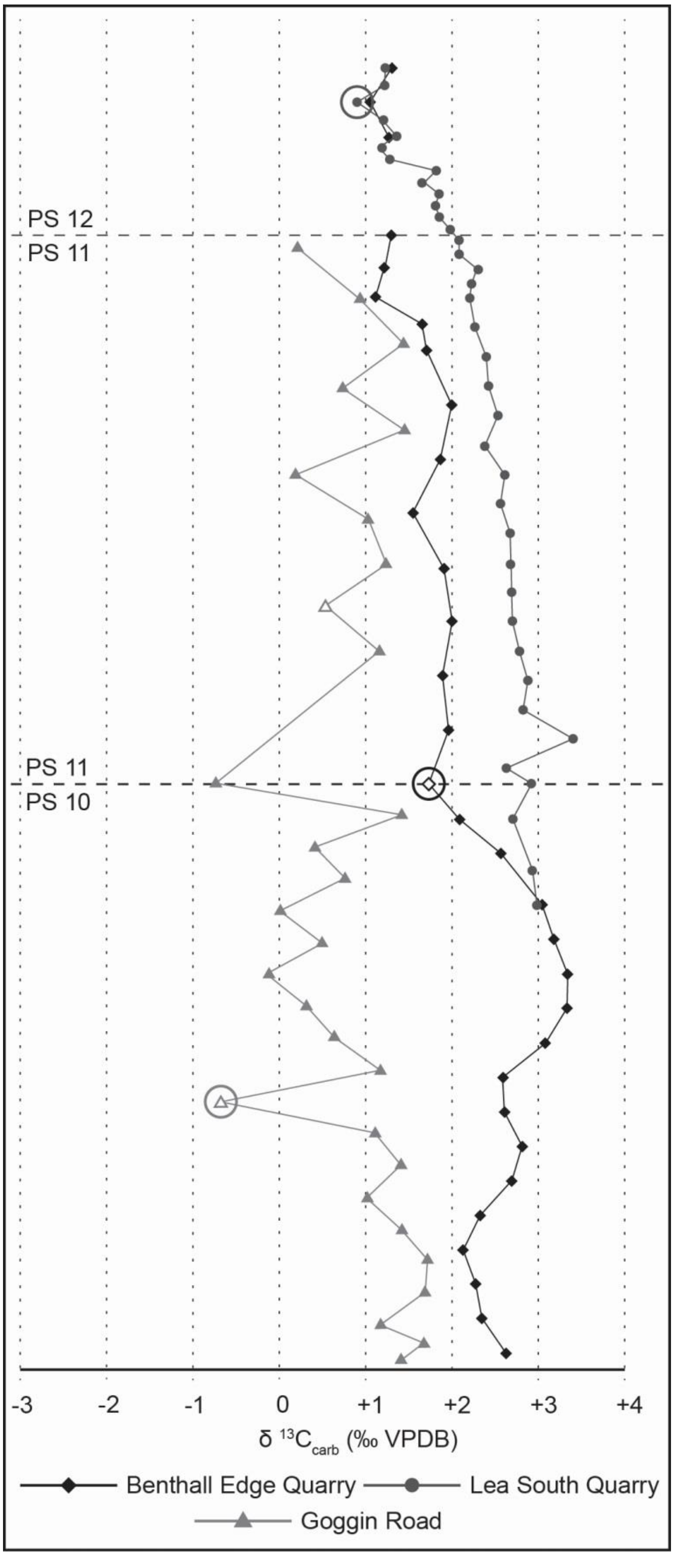
PS 12
PS 11
PS 11
PS 10
-3
-2
-1
0
+1
+2
+3
+4
δ 13Ccarb (‰ VPDB)
Benthall Edge Quarry
Lea South Quarry
Goggin Road

342

343

**Table S1.** $\delta^{13}C_{carb}$ and $\delta^{18}O$ data from Goggin Road, Lea South Quarry and Benthall Edge Quarry sections. Highlighted values (grey) denote samples which may have been affected by diagenesis.

**Goggins Road**

| Location | Position in section (m) | $\delta^{13}C_{carb}$ (‰ VPDB) | $\delta^{18}O_{carb}$ (‰ VPDB) |
|---|---|---|---|
| **PS 10** | | | |
| GR | 0.20 | 1.40 | -6.03 |
| GR | 0.40 | 1.65 | -5.16 |
| GR | 0.60 | 1.16 | -6.49 |
| GR | 0.80 | 1.68 | -6.41 |
| GR | 1.00 | 1.71 | -5.70 |
| GR | 1.20 | 1.40 | -6.82 |
| GR | 1.40 | 1.00 | -6.89 |
| GR | 1.60 | 1.39 | -5.59 |
| GR | 1.80 | 1.10 | -5.62 |
| GR | 2.00 | -0.69 | -8.64 |
| GR | 2.20 | 1.15 | -6.76 |
| GR | 2.40 | 0.62 | -6.69 |
| GR | 2.60 | 0.30 | -5.62 |
| GR | 2.80 | -0.12 | -7.44 |
| GR | 3.00 | 0.49 | -6.88 |
| GR | 3.20 | 0.00 | -5.19 |
| GR | 3.40 | 0.74 | -8.40 |
| GR | 3.60 | 0.40 | -7.20 |
| GR | 3.80 | 1.41 | -5.44 |
| **PS 11** | | | |
| GR | 4.00 | -0.76 | -4.74 |
| GR | 4.60 | 1.15 | -6.30 |

| Location | Position in Section (m) | $\delta^{13}C_{carb}$ (‰ VPDB) | $\delta^{18}O_{carb}$ (‰ VPDB) |
|---|---|---|---|
| GR | 4.80 | 0.51 | -7.65 |
| GR | 5.00 | 1.13 | -5.15 |
| GR | 5.20 | 1.03 | -5.76 |
| GR | 5.40 | 0.19 | -4.88 |
| GR | 5.60 | 1.43 | -5.63 |
| GR | 5.80 | 0.72 | -5.69 |
| GR | 6.00 | 1.42 | -5.09 |
| GR | 6.20 | 0.93 | -5.22 |
| GR | 6.40 | 0.22 | -5.33 |

**Lea South Quarry**

| Section | Position in section (m) | $\delta^{13}C_{carb}$ (‰ VPDB) | $\delta^{18}O_{carb}$ (‰ VPDB) |
|---|---|---|---|
| **PS 10** | | | |
| LS | 0.20 | 2.99 | -5.42 |
| LS | 0.60 | 2.94 | -5.93 |
| LS | 1.30 | 2.70 | -7.05 |
| **PS 11** | | | |
| LS | 1.70 | 2.92 | -4.75 |
| LS | 1.90 | 2.63 | -5.43 |
| LS | 2.30 | 3.40 | -4.96 |
| LS | 2.70 | 2.82 | -7.48 |
| LS | 3.10 | 2.86 | -5.66 |
| LS | 3.50 | 2.78 | -7.68 |
| LS | 3.90 | 2.70 | -7.64 |
| LS | 4.30 | 2.69 | -6.98 |
| LS | 4.70 | 2.69 | -6.56 |

| Location | Position in section (m) | $\delta^{13}C_{carb}$ (‰ VPDB) | $\delta^{18}O_{carb}$ (‰ VPDB) |
|---|---|---|---|
| LS | 5.10 | 2.67 | -5.70 |
| LS | 5.50 | 2.55 | -5.46 |
| LS | 5.90 | 2.60 | -7.50 |
| LS | 6.30 | 2.39 | -5.97 |
| LS | 6.70 | 2.53 | -6.31 |
| LS | 7.10 | 2.43 | -7.39 |
| LS | 7.50 | 2.40 | -7.74 |
| LS | 7.90 | 2.26 | -5.63 |
| LS | 8.30 | 2.20 | -5.89 |
| LS | 8.50 | 2.23 | -7.57 |
| LS | 8.70 | 2.26 | -7.39 |
| LS | 8.90 | 2.07 | -6.86 |
| LS | 9.10 | 2.07 | -5.81 |
| **PS 12** | | | |
| LS | 9.30 | 1.99 | -7.58 |
| LS | 9.50 | 1.85 | -5.77 |
| LS | 9.70 | 1.81 | -7.33 |
| LS | 9.90 | 1.84 | -7.36 |
| LS | 10.10 | 1.68 | -6.77 |
| LS | 10.30 | 1.82 | -6.83 |
| LS | 10.50 | 1.29 | -7.21 |
| LS | 10.70 | 1.15 | -6.46 |
| LS | 10.90 | 1.32 | -5.45 |
| LS | 11.10 | 1.16 | -6.15 |
| LS | 11.30 | 0.90 | -5.08 |
| LS | 11.50 | 1.22 | -5.24 |
| LS | 11.70 | 1.23 | -4.32 |

**Benthall Edge**

| Section | Position in section (m) | $\delta^{13}C_{carb}$ (‰ VPDB) | $\delta^{18}O_{carb}$ (‰ VPDB) |
|---|---|---|---|
| **PS 10** | | | |
| BE | 0.00 | 2.64 | -4.87 |
| BE | 0.40 | 2.35 | -5.66 |
| BE | 0.80 | 2.29 | -4.80 |
| BE | 1.20 | 2.14 | -5.18 |
| BE | 1.60 | 2.44 | -4.66 |
| BE | 2.00 | 2.70 | -4.61 |
| BE | 2.40 | 2.82 | -4.87 |
| BE | 2.80 | 2.62 | -4.20 |
| BE | 3.20 | 2.60 | -4.92 |
| BE | 3.60 | 3.09 | -4.30 |
| BE | 4.00 | 3.34 | -4.25 |
| BE | 4.40 | 3.35 | -4.35 |
| BE | 4.80 | 3.19 | -4.53 |
| BE | 5.20 | 3.05 | -4.28 |
| BE | 5.80 | 2.60 | -4.91 |
| BE | 6.20 | 2.12 | -6.62 |
| **PS 11** | | | |
| BE | 6.60 | 1.76 | -5.63 |
| BE | 7.00 | 2.00 | -4.22 |
| BE | 7.40 | 1.93 | -6.03 |
| BE | 7.80 | 2.04 | -4.23 |
| BE | 8.20 | 1.95 | -4.10 |
| BE | 8.60 | 1.58 | -4.84 |
| BE | 9.00 | 1.90 | -5.27 |

| | | | |
|---|---|---|---|
| BE | 9.40 | 2.03 | -6.07 |
| **Location** | **Position in Section (m)** | **$\delta^{13}C_{carb}$ (‰ VPDB)** | **$\delta^{18}O_{carb}$ (‰ VPDB)** |
| BE | 9.80 | 1.74 | -7.09 |
| BE | 10.00 | 1.68 | -6.06 |
| BE | 10.20 | 1.15 | -4.73 |
| BE | 10.40 | 1.25 | -6.20 |
| **PS 12** | | | |
| BE | 10.60 | 1.32 | -6.17 |
| BE | 11.80 | 1.30 | -4.76 |
| BE | 12.20 | 1.09 | -5.39 |
| BE | 12.60 | 1.34 | -7.50 |